Localized Hyperthermia with Electromagnetic Arrays and the Leaky-Wave Troughguide Applicator

CAREY M. RAPPAPORT, STUDENT MEMBER, IEEE, AND
FREDERIC R. MORGENTHALER, FELLOW, IEEE

Abstract—**Noninvasive microwave hyperthermia is an attractive cancer treatment modality. Understanding the advantages and limitations of focusing are vital for the practical implementations of electromagnetic heating of deep tumors. These, as well as the important issues of tissue coupling and proper choices of polarization and frequency are herein examined. An optimal theoretical source distribution and an applicator design that approximates this distribution are discussed.**

I. INTRODUCTION

MANY CANCEROUS TUMORS embedded in healthy human tissue have well-defined boundaries and tend to be irreversibly damaged by hyperthermia. Tumor temperature elevation to 43–46° C for 90 to 120 min appears to be sufficient to kill many types of malignant growths [1]–[3]. Several methods of delivery of heat to these localized tumors have been proposed [4]–[8], including capacitative and inductive RF source, single microwave source, focused ultrasound, invasive electromagnetic probe, and microwave array heating. Much of the current interest is with noninvasive sources, which are less traumatic to sick patients and minimizes the risk of mixing abnormal cells into healthy tissue.

The optimal noninvasive applicator delivers maximum power to the tumor while minimally heating surrounding healthy tissue. Since waves attenuate as they penetrate lossy tissue, a focusing source arrangement is required. Constructive interference at the tumor is obtained by adjusting the phase and amplitude of each point of the source. Unlike in free space, nearfield focusing in a lossy medium is more involved than simply compensating for the path length variations from tumor to source. Also, since the attenuation rate varies directly (though nonlinearly) with frequency, while field resolution decreases with decreasing frequency, any attainable "focus" is relatively wide and of low intensity. The broadening and smearing of this focal maximum increases as the physical distance in the medium to the source increases, until the exponential decay overwhelms any geometrical focusing advantages. For heating a tumor in the center of a volume of tissue, the best range of frequencies is found by choosing those patterns of dissipated power (if any exist) that have the same power at the focus as at the tissue surface with lower power for all intervening tissue, including muscle/fat boundaries. Generally, the sharpest focus or highest resolution will correspond to the highest possible frequency within this range of frequencies. Exceeding this range may produce higher resolution, but the actual penetration depth into the tissue will decrease.

More complicated than frequency selection is the determination of optimal source distribution. Unlike with the acoustic compression waves of ultrasound hyperthermia, electromagnetic waves incorporate polarization. For constructive interference at a focus, electric field at the tissue surface must be properly aligned and phased so that waves propagating along all paths in the entire tissue volume arrive in the same fashion. However, merely adjusting phase, polarization, and also amplitude for maximum focusing does not necessarily produce an acceptable power-density distribution. Consider Fig. 1 with a planar source on the left, with phase adjusted to focus on the point labeled F, 3 tissue wavelengths into the lossy medium. Although F is the only point of coherence in the tissue having significant gain over a uniform phase distribution, as shown in Fig. 1(b), the power there is still much lower than at points closer to the source, Fig. 1(c), which have a shorter exponential decay distance. These plots were calculated for muscle tissue at 915 MHz, with electrical parameters taken from Storm [4], using 32-point Gauss-Legendre integration of the diffraction integral.

Several experimental means of determining source distribution have been proposed. These include passive methods, such as remote sensing [9]; and active methods, such as invasive implantation of a small source at the intended focus, subsequent phase measurement at the surface and inversion for source specification. Both methods overlook the difficulty of undesirable hot spots or excessive surface heating, as shown in Fig. 1(c). Correcting the source distributions to prevent this often eliminates any geometrical advantage at the focus.

One further requirement of applicators is a method of monitoring power deposited in the exposed tissue. Applied

Manuscript received January 10, 1986, revised January 10, 1986. This work was supported in part by the National Cancer Institute, under Grant POl-CA 31303.

The authors are with the Department of Electrical Engineering and Computer Science, Massachusetts Institute of Technology, Cambridge, MA 02139.

IEEE Log Number 8607618.

0018-9480/86/0500-0636$01.00 ©1986 IEEE

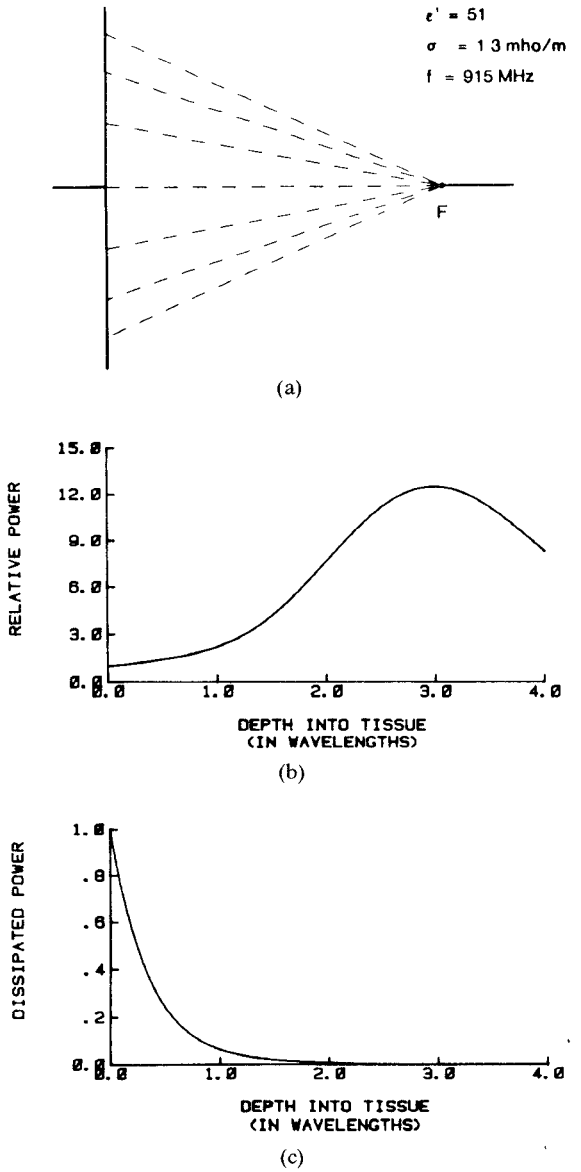

Fig. 1. Focusing at depth: Fallacy of maximum intensity at focus in a lossy medium. (a) Geometry. (b) Power gain over uniform plane wave. (c) Relative power density.

dosage information may be used as an approximate substitute for the difficult problem of direct noninvasive temperature measurement.

Although the effects of phase focusing a wave in tissue is not as great as in free space, advantage can be taken of a finite tissue volume by surrounding it with applicator sources. Two main simplified cases that yield good power patterns are examined in this study: planar arrays facing each other and cylindrical arrays. Their geometrical simplicity allows a harmonic wave analysis, which provides exact field solutions. The effects of phase focusing these source configurations is considered. Also, an applicator design that can be configured into these sources with power monitoring capability is presented.

II. Focusing in Lossy Tissue

To analyze the extent of focusing microwaves in biological tissue, the dielectric constant ϵ' and electric conductivity σ for the frequencies of interest must be known. The decaying wave in tissue is then represented by the wave number

$$k = \beta - j\alpha \tag{1}$$

where

$$\beta = k_o \left[\left(\left(\epsilon'^2 + \left(\frac{\sigma}{\omega \epsilon_0} \right)^2 \right)^{1/2} - \epsilon' \right) \Big/ 2 \right]^{1/2}$$

$$\alpha = k_0 \left[\left(\left(\epsilon'^2 + \left(\frac{\sigma}{\omega \epsilon_0} \right)^2 \right)^{1/2} + \epsilon' \right) \Big/ 2 \right]^{1/2}$$

$k_0 = \omega\sqrt{\mu_0 \epsilon_0}$, ω is the radian frequency, and $j = \sqrt{-1}$.

A plane wave, polarized in the y direction, is represented by

$$E_p(x, y, z) = \mathrm{Re}\left\{ \hat{y} \underline{E}_0(y, z) e^{-\alpha x} e^{-j\beta x} e^{j\omega t} \right\} \tag{2}$$

which decays in the positive x direction. An inwardly propagating cylindrical wave that is generated by an infinite cylindrical source is written

$$E_c(r, \varphi, z) = \mathrm{Re}\left\{ \hat{z} \underline{E}_0(\varphi, z) I_0((\alpha + j\beta) r) e^{j\omega t} \right\} \tag{3}$$

where I_0 is the zero-order modified Bessel function, which grows with increasing r in an approximately exponential fashion where r is large. The relative values of α and β determine the focusing resolution versus decay, whereas their absolute values give the physical penetration depth and focal spot size. The choice of polarization in (2) and (3) are vital. The electric fields of all sources must be parallel and must be transverse to the exposed tissue surface to ensure maximum constructive interference and field coupling between layers of different tissue. The latter principle is due to the continuity of tangential E-field as opposed to normal D-field. Transverse polarization is also desirable since it lessens the possibility of delivering excessive power and burning tissue on the low permeability side of a muscle/fat boundary, where the relative permeabilities abruptly lessen by a factor of about nine. Any normal electric-field component would be 9 times greater in the fat. And since conductivity is about 15 times less in fat than muscle, the dissipated power at the fat side of the boundary would be more than 5 times that of the muscle side.

Approximate values of the dielectric constant ϵ' and the conductivity σ for the two main types of biological tissue: muscle, or high water content; and fat, or low water content; as reported in the literature [4],[10]–[12] are plotted in Fig. 2. Note that near 2 GHz, the conductivity curve for muscle begins to rise rapidly. For frequencies above this range, the attenuation rate becomes too great for effective focusing at any useful depth.

Since many tumors are embedded in muscle tissue, and since muscle tissue is more lossy than fat and therefore more difficult to focus power at depth, the remainder of the study will be restricted to muscle tissue.

Using these values, the values of α and β are computed from (1), and power patterns can be determined using (2)

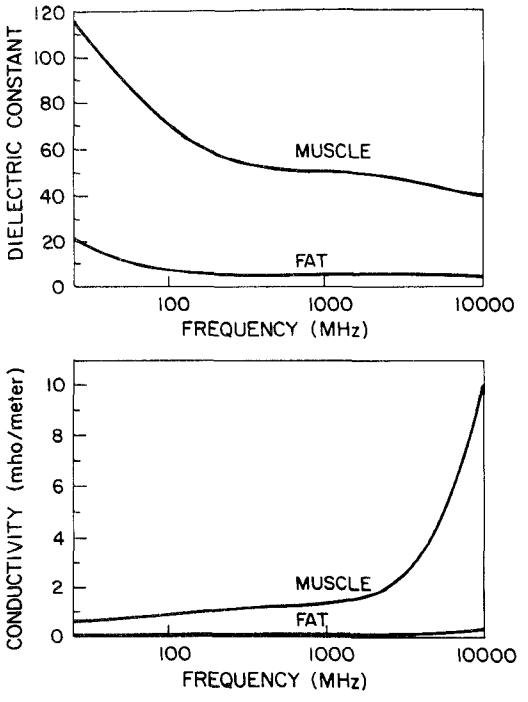

Fig 2. Electrical characteristics of high- and low-water content biological tissue as function of frequency (from [4]).

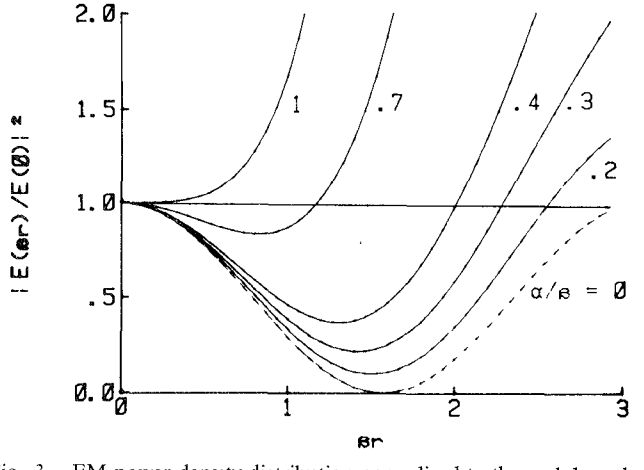

Fig. 3 EM power-density distribution normalized to the midplane density of an infinite planar slab of thickness $2r$, with uniform coherent source excitation, for typical values of α/β

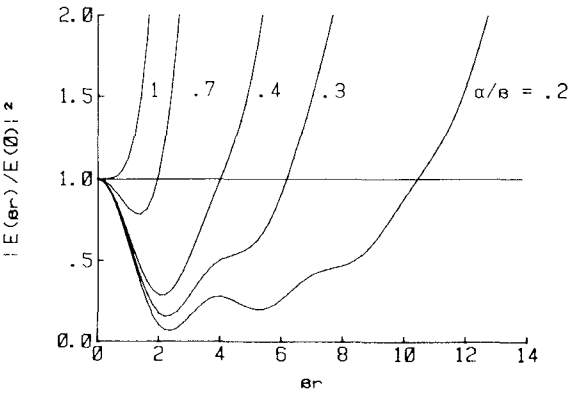

Fig 4. EM power-density distribution normalized to axis density for cylinder of radius r with uniform source excitation for typical values of α/β.

TABLE I
ATTENUATION TO PROPAGATION RATIO, TISSUE WAVELENGTH, AND MAXIMUM PENETRATION DIAMETER, AS A FUNCTION OF FREQUENCY, FOR MUSCLE TISSUE (FROM [4])

f(MHz)	α/β	WAVELENGTH IN TISSUE(cm)	DIAMETER D(max) in cm
27	.76	68	36
41	.732	51	29
100	648	27	19
433	.392	8.8	11.5
750	.271	5.3	11.8
915	.231	4.5	12.6
1500	.196	2.8	9.6
2450	.165	1.8	7 7

and (3). First, for two infinite, coherent planar sources, each facing an infinite slab of muscle tissue, the dissipated power, as a function of distance (normalized to tissue radian wavelength) is displayed in Fig. 3. Fig. 4 shows a similar plot for an infinite uniform cylindrical source surrounding an infinite rod of muscle tissue. For each case, the power levels are normalized to that at the center of the tissue. Applications of the planar arrangement are limited, but the cylindrical source can readily be used with arm, leg, or torso tissue volumes. In the former case, the requirement of equal power at the focus ($x = 0$, or the midplane of the tissue) and the surface determines the greatest uniform source separation distance. This distance ranges from more than $\beta x = 3.14$ for the lossless case to $\beta x = 1.2$ for $\alpha/\beta = 0.7$. The lossless example, though not of practical interest, illustrates the ideal optimal pattern and the extent of power reduction that must be considered when dealing with real, lossy tissue. This latter case approximately corresponds to 60-MHz sources separated by $x = 2.4\lambda/2\pi$, or about 21 cm. In Fig. 4, the radial distances where the power crosses unity are considerably greater than those of Fig. (3). For $\alpha/\beta = 0.2$, the maximum radius is almost four times the linear planar-source separation distance. Table I lists values of α/β for various frequencies and gives the maximum radii of cylinders of muscle tissue for which axial power equals surface power. At 915 MHz, a uniform infinite cylinder of muscle tissue, 6.3 cm in radius can have as much power deposited on its axis as on its surface, with a half-power radius of about 1 cm ($\beta r \approx 1.4$ from Fig. 4, $\beta = 2\pi/\lambda$, $\lambda = 4.5$ cm from Table I). This rather optimistic figure of course neglects asymmetries, tissue inhomogeneities, boundary mismatches, polarization discrepancies, and field-coupling losses found in actual imple-

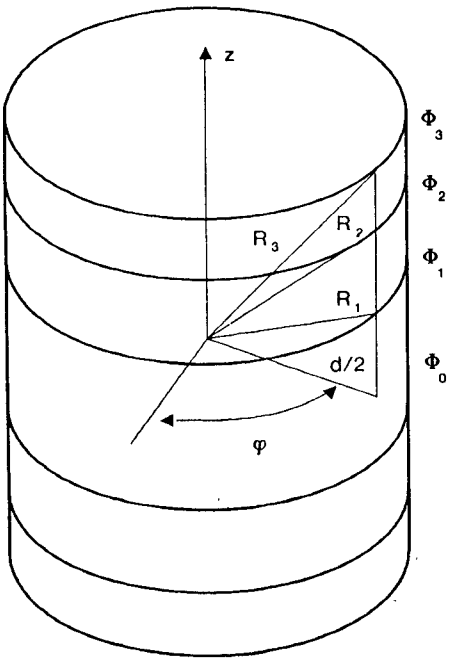

Fig. 5. Geometry of cylindrical focusing of axially polarized sources.

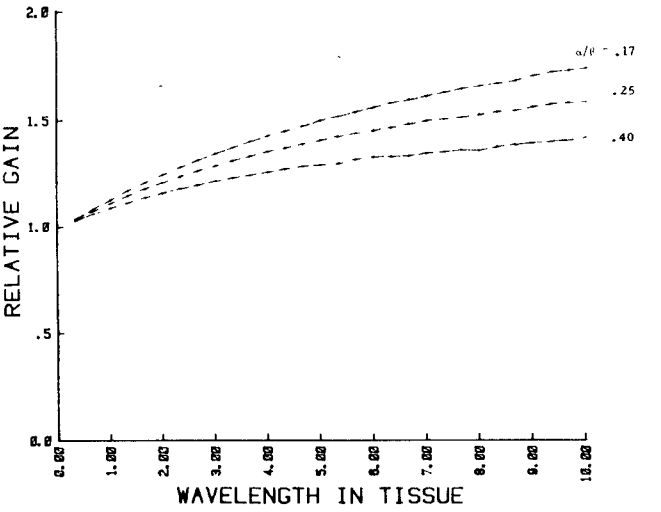

Fig. 6. Magnitude of gain of focused field over unfocused field for longitudinally $\hat{z}$ polarized source.

mentations. Also, being solely an electromagnetic analysis not considering thermal characteristics, it represents power density, rather than temperature rise. The practical, achievable maximum radius, based on temperature limitations, is undoubtedly less. The values of Table I are idealized limits only.

These maximum slab thicknessness and radii can be increased to some extent by surface cooling. Although skin is a very efficient insulator, and hence limits cooling effects to the order of millimeters, the power pattern and temperature profile tend to rise exponentially (see Fig. 1(c)) as they approach the skin surface. Constraining this portion of the profile has a large effect on the overall pattern.

Further focal depth increases can be realized by adjusting the source phase to compensate for differing path lengths to the focus. Fig. 5 illustrates the geometry of axial focusing in a cylinder. Each ring of constant z is given a phase $\Phi(z)$ such that the phase at the focus due to that ring is zero. Three typical rings are shown with phases Φ_i, with corresponding radial distances R_i, $i=1,2,3$. Since this is a near-field problem, the full Huygen–Kirchoff diffraction formula for the axial E-field must be used

$$\begin{aligned} E_z &= -j\omega\mu\left(\bar{\bar{I}}+1/k^2\nabla\nabla\right)\cdot\boldsymbol{A}\cdot\hat{z} \\ \boldsymbol{A} &= \int_{V'} dv' \frac{e^{-jk|r-r'|}}{4\pi|r-r'|}\boldsymbol{J}(r') \\ \boldsymbol{r} &= x\hat{x}+y\hat{y}+z\hat{z} \\ \boldsymbol{r}' &= x'\hat{x}+y'\hat{y}+z'\hat{z} \end{aligned} \tag{4}$$

where A is the magnetic vector potential, $J(r')$ is the electric-source distribution entirely directed in the z direction and limited to a cylindrical shell of radius $d/2$, $\bar{\bar{I}}$ is the identity matrix, and all source coordinates are primed. Applying the two gradient and the identity operations to the integrand inside the integral and integrating over φ' and ρ' yields a complex integral in z'. At the focus: $\rho=0$, $z=0$; this integral reduces to

$$E_z = \int_{-\infty}^{\infty} dz' A(z') e^{-j\Phi(z')} J(z') \tag{5}$$

where

$$A(z') = \frac{\omega\mu}{4\pi}\frac{e^{-\alpha R}}{R}\left(P^2+Q^2\right)^{1/2} \tag{5a}$$

$$\Phi(z') = \frac{\pi}{2}+\beta R-\tan^{-1}(Q/P) \tag{5b}$$

$$P = 1-\left(\frac{z'}{R}\right)^2+\left(3\left(\frac{z'}{R}\right)^2-1\right)\left(\frac{\beta^2-\alpha^2}{|k|^4R^2}-\frac{\alpha}{|k|^2R}\right) \tag{5c}$$

$$Q = \frac{\beta}{|k|^2R}\left(3\left(\frac{z'}{R}\right)^2-1\right)\left(1+\frac{2\alpha}{|k|^2R}\right) \tag{5d}$$

$$R = \left((d/2)^2+z'^2\right)^{1/2}. \tag{5e}$$

With uniform source amplitude, this integral is maximized for $J(z')=e^{j\Phi(z')}$. Note that this source distribution is more complicated than a focusing distribution in a lossless medium.

The integral (5) is approximated using $\alpha/\beta \ll 1$ and $\beta d/2 \gg 1$ and transformed into

$$E_z \propto \int_0^{\infty} d\tau \frac{1}{\cosh^2\tau} e^{-(\alpha d/2)\cosh\tau}. \tag{6}$$

This integral is equivalent to integrating $K_0(\alpha d/2)$ twice with respect to its argument using appropriate integration limits.

The unfocused field can be similarly approximated by replacing the α in (6) by $\alpha+j\beta$. The computed gain of focused E_z is plotted in Fig. 6 as a function of radius. For muscle tissue at 915 MHz, axial focusing increases the electric-field intensity by 1.5 times, more than doubling the power.

III. The Troughguide—A Leaky-Wave Antenna

One possible applicator design that radiates in a continuous and controlled fashion is the leaky-wave antenna. Essentially a waveguide with a radiating opening in its side or top wall, a leaky-wave antenna guides most of its power down its length. Boundary conditions for the interior propagating guided field at the opening are satisfied by a tangential E-field. Since the interior guided field propagates down the guide, the tangential E-field across the opening must have progressive linear phase. Thus, a nonuniform plane wave radiates at the angle from broadside specified by

$$\theta = \sin^{-1}(\lambda_0/\lambda_g) \tag{7}$$

where λ_0, and λ_g are the free-space and guide wavelengths, respectively.

Varying the size of the opening or adding obstructions in the guide near the opening changes the amplitude of the radiated field. For small openings and perturbations, the linear phase is not significantly affected. With the proper choice of continuous additions, a limited-extent uniform plane wave can be produced.

Unlike many other applicators, such as microstrip or horn antennas, radiated field interactions with lossy media do not change the basic field characteristics within the guide. Since the radiation is due to a relatively small perturbation, the guide wavelength and basic modal structure—and hence aperture phase—are unaffected by loading. Reflections from the load may affect aperture amplitude and must be minimized with adequate bolussing, but these primarily affect amplitude rather than phase. A leaky-wave applicator can be designed based solely on the surface currents specified theoretically, without knowledge of the particular medium being exposed.

The asymmetric troughguide, first reported in 1958 [13], is a leaky-wave antenna consisting of a U-shaped channel, open at the top, with a vertical center fin attached to its base and running down its length. The base on one side of the central fin is raised, introducing the asymmetry that generates a tangential E-field across the open top. A wide range of amplitude control is available by adjusting the relative height of the bases on each side of the fin. Reversing the asymmetry reverses the field, causing a 180° phase shift at the aperture. This configuration is shown in Fig. 7.

A primary advantage of the troughguide is the availability of power monitoring. Using short probes mounted at the points of high guide-E-field along the side wall and small loops along the base where H-field is strongest, these field quantities can be measured. Knowledge of both components is essential to avoid standing-wave ambiguities caused by reflections. With knowledge of the power as a function of distance within the guide, the radiated power between any two points is available. Since reflections are already taken into account with this monitoring, the measured radiated power is the actual power entering the exposed tissue. Few other applicators can claim this benefit.

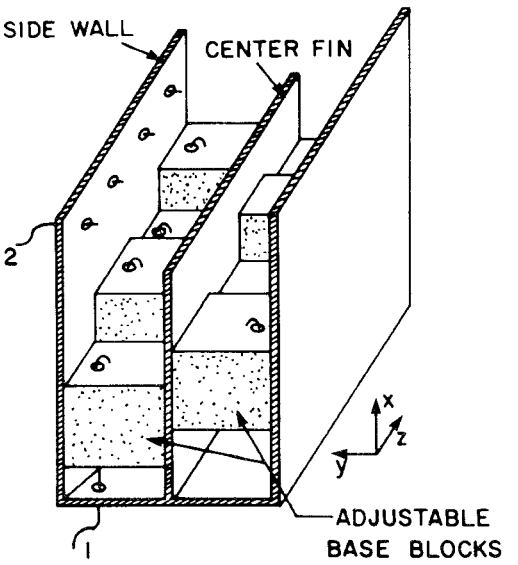

Fig. 7. Asymmetric troughguide with alternating base block asymmetries, H-field loops, 1 and E-field probes, 2.

For the troughguide described above, the aperture must be less than one half a wavelength wide. Filled with air and at 915 MHz, the aperture is less than 15 cm wide. Loading the antenna with a high dielectric reduces this width further. A stacked array of these narrow troughguide strips, each fed with proper phase, would closely approximate a continuous planar source. The E-field is always aligned perpendicular to the guide length, so stacking these guides gives a linearly polarized planar applicator. The amplitude is finely controllable over the entire array by the base positions in each guide.

IV. The Troughguide as a Hyperthermia Applicator

Real tissue is not uniform and cylindrical, and is often difficult to contact directly. A bolus filled with pure water or other liquid with dielectric constant close to that of biological tissue serves to smooth out irregularities. This liquid layer also can be used to cool the tissue surface. It is important to note that the power deposited in the bolus can greatly exceed that of the tissue, as long as this bolus heat is removed and the power near the tissue surface is minimized.

Unfortunately, due to layers of different tissue near the body surface, a bolus can never exactly match to interior muscle tissue. The problem of choosing the optimal dielectric liquid and its thickness to compensate for uneven intervening fat layers is likely to remain unsolved.

Minimizing the bolus thickness is desirable for several reasons. For a thinner layer, waves have less of a chance to spread, and diffraction and reflection effects are smaller. Further, the cancelling of field between adjacent unequally-phased array elements is most prominent nearest the applicator. This is a benefit near the tissue surface that should not be entirely wasted in the bolus layer. One last advantage of a thin layer is the greater confidence of predicting power deposition in tissue. The troughguide monitoring scheme only measures power leaving the appli-

cator. With a thick bolus layer, the correspondence between the point where power leaves the applicator to the point where power enters tissue is less certain.

In the planar configuration, besides setting the phases of adjacent guides, focusing can also be improved by simulating a Fresnel zone arrangement in each guide. Alternating the base asymmetry as shown in Fig. 7, with properly chosen lengths of base sections, can increase power at the focus by almost a factor or two. Thus, adjusting phase for focusing in both y and z directions increases power an additional factor of two according to Fig. 6 up to four times the uniform case.

The block lengths for the Fresnel configuration must be chosen with the tilted wavefront in mind. Block asymmetry is reversed each time the path length times the propagation constant β added to the applicator field phase increases by half a tissue wavelength. Unlike the usual case, the Fresnel zones are not symmetric about the focus.

Another applicator design consists of bending the planar array about an axis parallel to the tangential aperture E-field into a cylinder. Each guide section is a ring, though not completely closed to allow for a source and load region. As previously described, these stacked rings, each at a different z' height, are fed with waves phased according to (5b) to yield an axially focused cylindrical applicator. Of course with this arrangement, there are no base alterations, although the relative heights would be varied to maintain uniform amplitude. The progressive phase along the guide ring prevents this applicator from being uniform and does lessen the focusing effect. The field at the axis is reduced by the amount $\sin(\pi a)/\pi a$, when the progressive phase is $\Phi(\varphi) = a\varphi$.

V. Conclusions

Electromagnetic hyperthermia offers a promising modality for treating cancer in humans. Important aspects including polarization, depth of heating, power profile resolution, secondary power maxima, and source distribution must be given careful consideration. Attempts have been made to synthesize power patterns and specify the maximum planar and cylindrical muscle dimension for practical heating. Using a modal scheme on simplified geometries, followed by phase correction improvement—rather than experimental inverse phase specification—leads to a pattern less likely to have hot spots.

The optimal cylindrical source was shown to be polarized in the axial z direction, have no phase variation in φ, and phase variation $\Phi(z)$ according to (5b).

An applicator was suggested based on an array of asymmetric troughguide antennas, which produces a controllable transversely polarized leaky wave. As a bound-mode structure, the radiation characteristics are weakly affected by lossy tissue loading. There exist adjustments to minimize reflections; and propagating (and hence radiating) power can be easily monitored. This applicator can be designed to closely simulate the theoretically optimal cylindrical configuration.

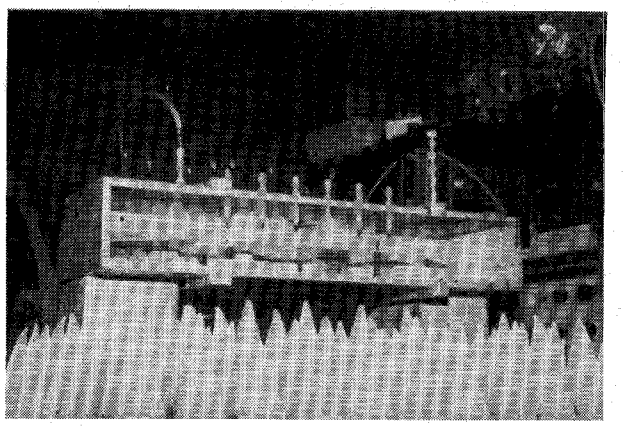

Fig. 8. Experimental linear troughguide setup.

Experiments are progressing with the troughguide antenna, Fig. 8. This linear antenna element is tested at 915 MHz, with the appropriate phantom material simulating lossy muscle tissue [14]. From this view into the top troughguide opening, six pairs of adjustable base blocks are visible, as are the E-field probes and H-field loops.

In many ways, this antenna is an improvement over currently used applicators. It has most of the advantages of microwave horns without the necessity of dielectric loading. The troughguide is an electrically flexible linear array, and thus simplifies the power-splitting and phase-shifting feed network. It also has a novel nonperturbing power monitoring capability. With all these advantages, the troughguide appears to be a good candidate for a microwave hyperthermia applicator.

Appendix
Design Equations for the Troughguide

A summary of the design method presented by Rotman and Naumann [13] follows.

The complex transcendental equation which describes the matched transverse resonance within the troughguide is

$$\tan(w) + \tan(pw) = 2j \tag{A1}$$

where

$$w = \left[k_0^2 + (\alpha_g + j\beta_g)^2\right]^{1/2}[s_1 + \delta] \tag{A2}$$

$$w = u + jv$$

$$p = \frac{s_2 + \delta}{s_1 + \delta} \tag{A3}$$

$$\delta = \frac{1}{2\pi}\left[(4\ln 2)b + \lambda_c \sum_{n=1}^{\infty}\left(\sin^{-1}\frac{4b}{n\lambda_c} - 2\sin^{-1}\frac{2b}{n\lambda_c}\right)\right]. \tag{A4}$$

α_g is the attenuation per unit length of the guided wave and $\beta_g = 2\pi/\lambda_g$ is the guide propagation constant, with b, s_1, and s_2 identified in Fig. 9, and with λ_c to be determined later. Also, from (7), the guide wavelength in terms of frequency f, radiation angle θ, and the speed of light c, is

$$\lambda_g = \frac{c/f}{\sin\theta}. \tag{A5}$$

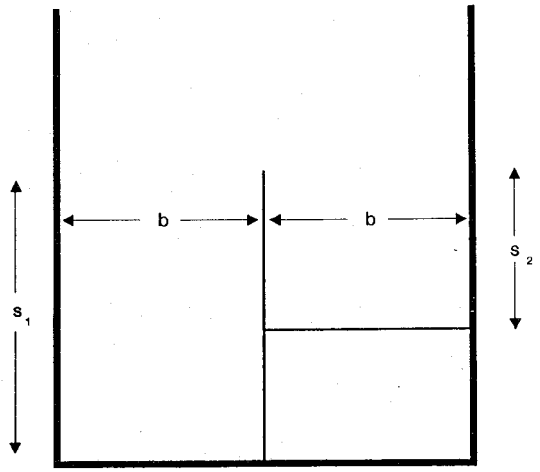

Fig. 9. Asymmetric troughguide: Typical element geometry.

Equation (A1) is numerically solved in terms of p, with the intermediate variables $u(p)$ and $v(p)$ uniquely determined from its real and imaginary parts.

The guide attenuation constant is found by solving the real and imaginary parts of (A2) which gives

$$\alpha_g = \frac{u^2 - v^2}{2uv}\beta_g - \left[\left(\frac{u^2 - v^2}{2uv}\beta_g\right)^2 - K^2\right]^{1/2} \tag{A6}$$

where $K^2 = k_0^2 - \beta_g^2$, and $k_0 = 2\pi/\lambda_0$. Equation (A6) and the definition of troughguide cut-off wavelength are now combined to give

$$\lambda_c = 2\sqrt{2}\,\pi\left[\alpha_g^2 + K^2 - \left(\left(\alpha_g^2 + K^2\right)^2 + 4\alpha_g^2\beta_g^2\right)^{1/2}\right]^{-1/2} \tag{A7}$$

which gives a value for δ from (A4). Given values of u, v, α_g, and δ, s_1 is given by

$$s_1 = \left(\frac{uv}{\alpha_g\beta_g}\right)^{1/2} - \delta \tag{A8}$$

and s_2 follows from (A3).

Although it would be preferable to solve these equations in terms of α_g, (A6) cannot be inverted, since both u and v cannot be determined by a single real equation.

Acknowledgment

The authors wish to thank C. Chiang for her careful computer manuscript preparation.

References

[1] G. M. Hahn, "Hyperthermia for the engineer: A short biological primer," *IEEE Trans. Biomed. Eng.*, vol. BME-31, no. 1, pp. 3–8, Jan. 1984.

[2] K. Overgaard, and J. Overgaard, "Investigations on the possibility of a thermic tumor therapy-1," *Euro. J. Cancer*, vol. 8, pp. 65–78, 1972.

[3] J. B. Marmor, N. Hahn, and G. M. Hahn, "Tumor cure and cell survival after localized radiofrequency heating," *Cancer Res.*, vol. 37, pp. 879–883, Mar. 1977.

[4] F. K. Storm, Ed., *Hyperthermia in Cancer Therapy*. Boston, MA: Prentice–Hall, 1983.

[5] G. M. Samaras and A. Y. Cheung, "Microwave hyperthermia for cancer therapy," *CRC Critical Rev. Bioeng.*, pp. 123–184, Feb. 1981.

[6] D. A. Christensen and C. H. Durney, "Hyperthermia production for cancer therapy: A review of fundamentals and methods," *J. Microwave Power*, vol. 16, no. 2, pp. 89–105, 1981.

[7] P. P. Lele, "Induction of deep, local hyperthermia by ultrasound and electromagnetic fields," *Radiation Environ. Phys.*, vol. 17, pp. 205–217, 1980.

[8] R. J. Dickinson, "An ultrasound system for local hyperthermia using scanned focussed transducers," *IEEE Trans. Biomed. Eng.*, vol. BME-31, no. 1, pp. 120–125, Jan. 1984.

[9] T. Tsang, J. A. Kong, and R. T. Shin, *Theory of Microwave Remote Sensing*. New York: John Wiley, 1985.

[10] C. C. Johnson and A. W. Guy, "Nonionizing electromagnetic wave effects in biological materials and systems," *Proc. IEEE*, vol. 60, no. 6, pp. 692–718, June 1972.

[11] H. P. Schwan and K. R. Foster, "RF-field interactions with biological systems: Electrical properties and biophysical mechanisms," *Proc. IEEE*, vol. 68, no. 1, pp. 104–113, Jan. 1980.

[12] K. R. Foster and J. L. Schepps, "Dielectric properties of tumor and normal tissues at radio through microwave frequencies," *J. Microwave Power*, vol. 16, no. 2, pp. 107–119, 1981.

[13] W. Rotman and S. J. Naumann, "The design of trough waveguide antenna arrays," ASTIA Document No. AD152427, AFCRC-TR-58-154, Air Force Cambridge Res. Center, June 1958.

[14] A. W. Guy, "Analyses of electromagnetic fields induced in biological tissues by thermographic studies on equivalent phantom models," *IEEE Trans. Microwave Theory Tech.*, vol. MTT-19, no. 2, pp. 205–214, Feb. 1971.

✠

Carey M. Rappaport (S'81) received the B.S. degree in mathematics, the B.S., M.S., and Engineers degrees in electrical engineering, all in 1982, from the Massachusetts Institute of Technology, Cambridge, MA. He is pursuing the Ph.D. degree in electrical engineering at MIT.

From 1978 until 1983, he spent summers working cooperatively at COMSAT Laboratories in Clarksburg, MD. His research involved reflector design, antenna measurements, and computer simulation of spacecraft antennas. During 1984, Mr. Rappaport examined sparsely-filled array antenna grating lobe reduction at the Aerospace Corp. in El Segundo, CA. Since 1981, he has served as a teaching assistant and research assistant for MIT's Department of Electrical Engineering and Computer Science. His current research involves antenna design for microwave hyperthermia cancer therapy.

Mr. Rappaport is a member of Eta Kappa Nu and Sigma Xi honorary professional societies.

✠

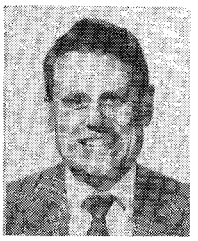

Frederic R. Morgenthaler (F'78) received the S.B. and S.M. degrees in electrical engineering in June 1956 and the Ph.D. degree in June 1960, from the Massachusetts Institute of Technology.

He is a Professor of Electrical Engineering at MIT and currently holds the Cecil H. Green Professorship for 1984–86. During the academic years 1960 to 1962, he was a Ford Foundation Postdoctoral Fellow in Engineering and an Assistant Professor in the MIT. Department of Electrical Engineering. In 1965, he was promoted to the rank of Associate Professor and in 1968 to the rank of Professor. A member of the Research Laboratory of Electronics, the Center for Materials Science and Engineering, and Director of the Microwave and Quan-

tum Magnetics Group, he also holds an appointment to the Harvard-MIT Division of Health Sciences and Technology. His research and graduate teaching has centered on the fields of microwave magnetics and ultrasonics, the electrodynamics of waves and media, and microwave signal processing using coherent wave states in solids. He is currently active in the field of magnetic recording. In addition, Dr. Morgenthaler participates in an interdisciplinary course in medical and industrial ultrasonics He also has taught the undergraduate electrical engineering core curriculum subjects in electromagnetic field theory, circuit theory, and semiconductor electronics. He was in charge of the field theory course from 1965–1968 and lecturer in charge of the transistor course from 1973–1978. Dr. Morgenthaler serves as a consultant to the U.S. Government as well as to private industry. He is the author of numerous scientific publications and papers presented at technical conferences and has been granted approximately 12 patents with several others pending. Dr. Morgenthaler is a member of the American Physical Society, the American Association for the Advancement of Science, and of the Sigma Xi, Tau Beta Phi, and Eta Kappa Nu honorary professional societies.